

A *ab initio* theory of nanoscale capacitors at finite bias

Massimiliano Stengel¹ and Nicola A. Spaldin¹

¹Materials Department, University of California, Santa Barbara, CA 93106-5050, USA
(Dated: February 19, 2019)

We present a novel technique for calculating the properties of an electric field applied to a periodic heterostructure with alternating metallic and insulating layers. This scheme allows us to investigate fully from first-principles the microscopic properties of a thin-film capacitor at finite bias potential. We demonstrate how the capacitance and local permittivity profiles can be readily obtained by performing a series of calculations for the Ag(100)/MgO(100) system. Applications range from the emerging field of electronic devices based on ferroelectric materials, to the *ab initio* simulation of electrochemical cells.

PACS numbers: 71.15.m

The dielectric response of a metal-insulator interface to an applied electric field is a subject of great interest nowadays, as the ongoing miniaturization of electronic devices is reaching the atomic scale. In this regime, the properties of thin oxide layers (used e.g. in nonvolatile ferroelectric memories [1] and as gate oxides in MOSFET transistors [2]) start to deviate from those predicted by macroscopic models, and cannot be disentangled from the metallic or semiconducting contact [3]. One particularly important issue related to interfacial effects is the "dielectric dead layer" [4], which plagues the performance of thin ferroelectric capacitors by substantially reducing the effective size of the active high- κ material. Interface chemistry [5], finite screening length in the metal [6], or the presence of structural and point defects could each be responsible for the experimentally observed permittivity depletion, but a generally accepted explanation is still missing. In order to separate these effects and to help improve over the existing models, the electronic and ionic response of a metal-insulator heterostructure to an external bias potential must be understood at the quantum mechanical level.

First-principles calculations, especially within the framework of density functional theory, have proven to be a powerful tool in the fundamental understanding of metal-ceramic interfaces [7]. On the other hand, *ab initio* studies of interfacial dielectric properties are still in their infancy, and only insulating heterostructures have been successfully simulated [5] in a finite external field. Indeed, when one of the two materials is a metal (as required for the simulation of a realistic thin-film capacitor), the presence of partially filled bands at the Fermi level prevents the straightforward application of the Berry phase technique [8], on which most finite electric field calculations have been based so far [9, 10]. In order to gain further insight into the rich domain of phenomena occurring at metal-dielectric junctions there is the clear need for a methodology that allows one to work around this obstacle.

In this work we demonstrate how this problem can be solved by using techniques and ideas borrowed from the

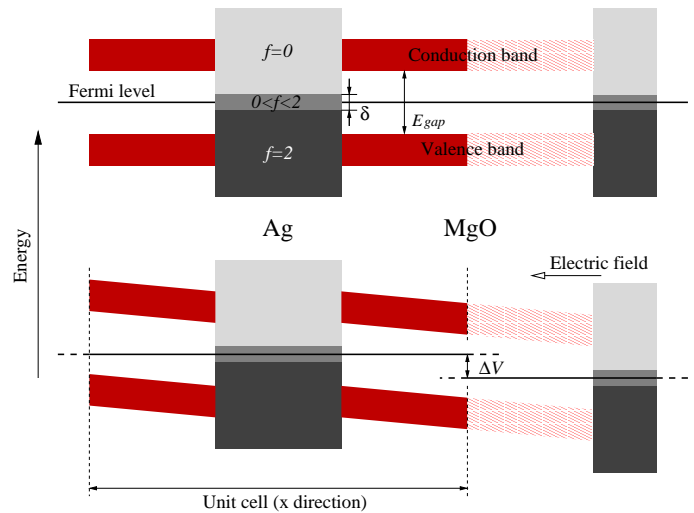


FIG. 1: Schematic representation of the projected band structure of a metal-insulator heterostructure in absence (top) and with (bottom) electric field. An effective bias potential ΔV between one slab and the repeated images is obtained.

Wannier functions theory, which is an appealing alternative to the traditional Berry-phase formalism [11]. In our method, the expectation value of the position operator is written in terms of "hempaphrodite" orbitals [12] (i.e. wavefunctions that are localized along the field direction and Bloch-like in the plane normal to it), which are obtained by an appropriate unitary transformation within the fully occupied submanifold. The electric field operator acts then as a state-dependent saw-tooth potential that polarizes the system along the field direction. We demonstrate our technique by performing numerical tests on the MgO/Ag(100) system, where we investigate the static and high-frequency dielectric and polarization profiles, and the electronic contribution to the capacitance as a function of thickness. Finally we show, by performing sample molecular dynamics runs within a finite bias voltage, that microcanonical simulations can be performed with high accuracy, thus opening the way to a wide range of finite-temperature applications.

Modern theory of polarization relates the macroscopic polarization of an insulating material to the centers of the Wannier functions [8] (WFs); potential use of the WFs to couple a periodic system to a uniform external field has been already demonstrated [13, 14]. Whenever the problem is one-dimensional, e.g. for a layered heterostructure, it is most practical to work with "hermaphrodite" orbitals [12, 15] rather than with proper WFs; the former are optimally localized along the field direction (which will be indicated as x from now on) and Bloch-like in the yz plane normal to it (in the remainder of the paper, when speaking of Wannier functions we will always refer to hermaphrodite ones). In order to use WFs in a finite field calculations there are three distinct steps that must be addressed: i) the unitary transformation of Bloch states that yields the required set of localized orbitals must be constructed; ii) the centers of the resulting WFs has to be defined to construct an appropriate expression for the polarization; iii) the energy term and the electric field operator must be defined and incorporated in the total electric enthalpy and the Hamiltonian, respectively.

Concerning step i), a one-dimensional localized representation is straightforward to enforce in an insulator by means of the "parallel transport" algorithm [16]. In metallic systems, however, unitary transformations are notoriously a delicate issue. In particular, when a Fermi level broadening is adopted, the energy functional is not invariant under an arbitrary rotation of the wavefunctions unless the occupation matrix f undergoes the same transformation [17]; since it is very desirable to work in the representation where f is diagonal, at first sight we're facing a serious limitation. Here we overcome it by dividing the problem into three regimes (a schematic representation is shown in Fig. 1):

The completely empty states with zero occupation numbers are discarded from the computation, since they do not contribute to the ground state energy or charge density.

The partially occupied states in the region of the Fermi level (shown in gray in Figure 1) are strictly contained in the energy gap of the dielectric, provided that a small enough smearing temperature is chosen. This means that these are metal-induced gap states (MIGS), i.e. they are already exponentially localized along the x direction without taking any further action since they do not propagate through the insulator.

The submanifold of fully occupied valence states (with energy eigenvalue $E_n < E_F$ in Fig. 1) is localized separately by means of the parallel-transport algorithm [16]; this operation leaves the total energy and the occupation matrix unaffected.

Having defined a suitable representation where all the electronic states are localized along the field direction, we can now address step ii) and write an expression for the polarization along x :

$$\mathbf{hP}_i = \frac{1}{V} \left(\sum_n f_n \mathbf{r}_n + \sum_I q_I \mathbf{R}_I \right); \quad (1)$$

where V is the volume of the supercell, f_n is the occupancy of the n -th WF, q_I is the charge of I -th pseudopotatom and \mathbf{R}_I its position along x ; the brackets indicate averaging over the cell. The Wannier centers \mathbf{r}_n are obtained by using periodic sawtooth functions, in a spirit close to that of Ref. [18]. In particular, first a point \mathbf{x}_n in the cell is determined for each Wannier function where the planar average of the individual Wannier density $n(\mathbf{x})$ has the smallest value [27]. Then we define:

$$\mathbf{r}_n = \frac{\int_{\mathbf{x}_n}^{\mathbf{x}_n+L} n(\mathbf{x}) d\mathbf{x}}{\int_{\mathbf{x}_n}^{\mathbf{x}_n+L} d\mathbf{x}}; \quad (2)$$

and we further impose $\mathbf{r}_n \in [0, L]$ to obtain a single well-defined value.

Finally, concerning step iii), the coupling with a finite external field adds a term to the Kohn-Sham total energy E_{KS} which provides the electric enthalpy E^E :

$$E^E = E_{KS} + V E \mathbf{hP}_i \quad (3)$$

The contribution \mathbf{hP}_i to the Hamiltonian due to the electric field operator is written as a non-local, state-dependent polarizing potential $F_n(\mathbf{x})$ applied to each WF (indicated hereafter as w_n) individually:

$$\mathbf{hP}_i = E \sum_n \hat{f}_n w_n i \hbar w_n j; \quad (4)$$

These $F_n(\mathbf{x})$ are sawtooth functions in real space [28], chosen so that they intersect the origin $x = 0$, but with state-dependent discontinuities in the points $x = x_n$ where each orbital has vanishing importance [29]. This particular vertical alignment is dictated by the necessity of respecting the correct limit in the special case of an isolated slab in vacuum (where the field operator can be made local) [19]. At first sight an undesirable side effect appears though, in that when a center \mathbf{r}_n crosses the point $x = L/2$ (the center of the insulating slab), the corresponding polarizing potential $F_n(\mathbf{x})$ undergoes a discontinuous, rigid jump of absolute magnitude $V = EL$. For a sufficiently thick insulating layer, and as long as V is small enough not to bring valence or conduction states into the partially occupied region close to the Fermi level, this jump leaves the system unaffected apart from a trivial shift of the total energy by a quantum of polarization. Interestingly, the large field Zener instability reported for purely insulating bulk materials [9, 10] translates here to a Schottky-tunneling

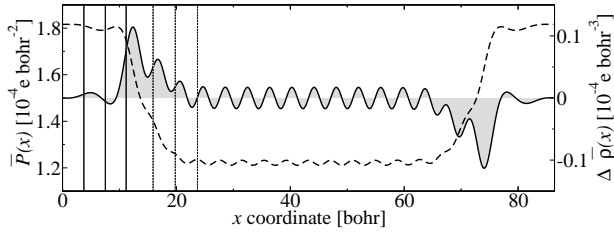


FIG. 2: Induced charge (solid filled curve) and polarization profile P (dashed curve) for the 15L M gO / Ag system. A Gaussian filter of width 2.0 bohr was used along x .

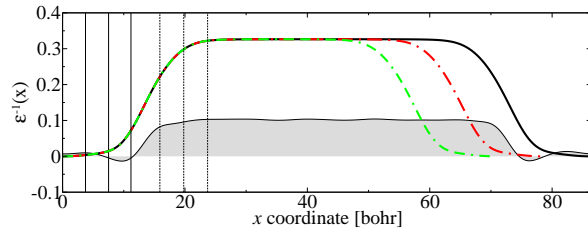


FIG. 3: Inverse permittivity profiles for the M gO thin-film capacitor. We compare the electronic response as a function of thickness (thick curves), and the static response for the 15L M gO case (thick dashed curve). A Gaussian broadening of 4.0 au. along x was used for all profiles.

instability that has to be avoided by careful analysis of the band alignment [30].

By the above strategy, we have obtained a polarized capacitor, with a finite bias potential $V = EL$ induced between one plate and the neighboring repeated image. Of course, the first property one might want to calculate is its capacitance density $C = -V$, where V is the density of the free charge stored on the plate. At first sight, one may be tempted to assume that V is simply the integral of the interfacial charge accumulation/depletion induced by the electric field (see Fig. 2). This is however physically incorrect, since this latter quantity includes a substantial contribution from the polarization charge density of the dielectric. Instead, V is uniquely defined as the time integral of the transient current that flows through the circuit while the electric field is adiabatically switched on; this corresponds exactly to the definition of macroscopic polarization differences [11]. We note that in a layered system the macroscopic polarization is nonuniform across the cell, and assumes different average values in the two materials due to their different response to the field. For the present derivation we need the polarization $P(x)$ (from now on, the bar indicates both planar averaging and Gaussian filtering along x) deep in the metal, i.e. for $x = 0$; if the metallic slab is thick enough, the middle region remains unperturbed by the field and plays the role of the conducting wire in a realistic circuit. $P(x)$ can be readily obtained from the induced charge density

Thickness (M gO layers)	C (actual)	C_0 (nominal)
11	0.00575	0.00568
13	0.00485	0.00481
15	0.00420	0.00417

TABLE I: Evolution of the (high frequency) capacitance per surface unit C for the unrelaxed Ag/M gO (100) heterostructure. The nominal values are obtained by using $C_0 = -V/d$, where d is the nominal thickness of the dielectric.

(x):

$$\langle x \rangle = \langle \epsilon_e(x) \rangle_0(x) \quad (5)$$

by using the classical definition:

$$\frac{dP(x)}{dx} = \langle x \rangle; \quad (6)$$

where $\epsilon_e(x_0)$ indicate the ground state charge density with (without) external field. The unknown integration constant in $P(x)$ is the total average polarization per supercell P as defined by Eq. 1 (an example of induced charge and corresponding polarization profile is shown in Fig. 2). Finally one obtains the capacitance density:

$$C = \frac{P(0)}{EL}; \quad (7)$$

From the same quantity $P(x)$, it is easy to extract the local permittivity profile $\epsilon(x)$ across the cell through the formalism developed in Ref. 15, which is equally valid for both the high-frequency and static response of the device (in our tests we will make use of Eq. 8, pag. 2).

We demonstrate the effectiveness of our scheme by presenting results for the Ag(100)/M gO (100) interface [31]. In all calculations we used a seven-layer Ag slab, with starting atomic positions taken from a fully relaxed isolated slab. Assuming an interfacial distance of 2.5 Å, we then completed the supercell by adding an appropriate number (11-15) of M gO layers set initially in the ideal bulk positions.

First, we checked the evolution of the electronic contribution to the capacitance as a function of M gO thickness (i.e. without relaxing the atomic positions). We report in Table I the results for the calculated frozen-ion capacitance, which compare very well to the nominal values. For the same system we extracted the local permittivity profiles, which are reported in Fig. 3; these show that the calculated bulk dielectric constant of M gO (3.06) is recovered quite quickly, and the transition to metallic screening is relatively abrupt. This indicates, perhaps surprisingly, that the influence of the metal on the (high-frequency) dielectric properties of the M gO layer is very small. As expected, the permittivity diverges in the metallic region. The comparison between the 11, 13 and 15 layer-thick M gO film indicates a smooth and consistent permittivity profile in all cases, even in the thinnest

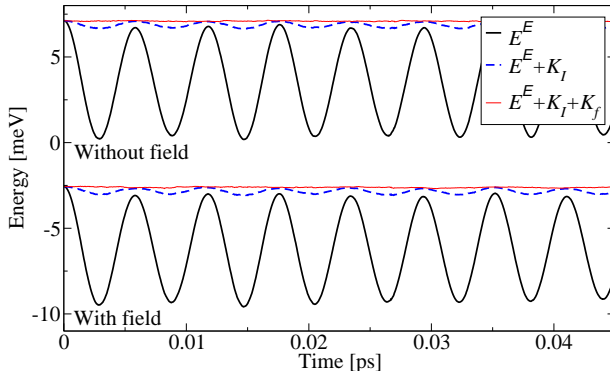


FIG. 4: Energy conservation for two microcanonical runs with (bottom curves) and without (top curves) electric field. Represented are the electric enthalpy (total energy) E^E , the "physical" constant of motion $E^E + K_I$ and the approximate "mathematical" constant of motion $E^E + K_I + K_f$, where K_I and K_f are the ionic and "fake" electronic kinetic energy respectively (see Ref. 20 for an overview of the method). The zero of the energy scale is set at the ground state total energy of the fully relaxed structure in zero field.

one where the overlap between the tails of the MIGS is more important and numerical accuracy could become an issue. Next, we fully relaxed the largest structure (with 15 MgO layers) separately in zero field and with applied electric field (we used $E = 0.0005$ a.u.), and extracted and compared the zero- and high-frequency permittivity profiles. ϵ_1 stayed close to its unrelaxed value (apart from a very minor interface buckling the effects of zero-field relaxation were negligible), while ϵ_0 in the MgO slab converged quickly to a value of 9.8. Finally, we performed a molecular dynamics simulation with and without electric field, in order to assess the quality of the dynamics. We note that within the extension of the Car and Parrinello method [21] to metallic systems [20, 22], a mathematical constant of motion is not easily available, in contrast to the insulating case. Some insight can nevertheless be gained by comparing similar runs with and without electric field switched on. For the run without (with) electric field we started from the atomic positions obtained by fully relaxing the system with (without) electric field, and we allowed the atoms to evolve freely along the x axis. In Fig. 4 we show the evolution of the relevant quantities as a function of time. It is evident from the figure that the quality of energy conservation is practically identical in the two cases.

In conclusion, we have presented a new scheme for performing ab-initio simulations within a finite electric field, and we have demonstrated its usefulness by performing test calculations on thin- $\text{Ag}(100)/\text{MgO}(100)$ capacitor. Our formalism is directly applicable to ferroelectric capacitors, for which extensive studies are being made experimentally, but many details are still poorly understood. The quality of overall energy conservation sug-

gests the feasibility of ab-initio electrochemistry, which could be obtained by replacing the insulating solid with an ionic solution.

This work was supported by the National Science Foundation's Division of Materials Research through the Information Technology Research program, grant number DMR-0312407, and made use of MRL Central Facilities supported by the National Science Foundation under award No. DMR-0080034

- [1] C. H. Ahn, K. M. Rabe, and J.-M. Triscone, *Science* **303**, 488 (2004).
- [2] K. Eisenbeiser, J. M. Finder, Z. Yu, J. Ramdani, J. A. Curless, J. A. Hallmark, R. D. Roopad, W. J. Ooms, L. Salem, S. Bradshaw, et al., *Appl. Phys. Lett.* **76**, 1324 (2000).
- [3] M. D. Dawber, K. M. Rabe, and J. F. Scott, cond-mat/0503372 (2005).
- [4] C. Zhou and D. M. Newns, *J. Appl. Phys.* **82**, 3081 (1997).
- [5] F. Giustino, P. Umari, and A. Pasquarello, *Phys. Rev. Lett.* **91**, 267601 (2003).
- [6] J. Junquera and P. G. de Gennes, *Nature* **422**, 506 (2003).
- [7] M. W. Finn, *J. Phys.: Condens. Matter* **8**, 5811 (1996).
- [8] R. D. King-Smith and D. Vanderbilt, *Phys. Rev. B* **47**, R1651 (1993).
- [9] I. Souza, J. Iñiguez, and D. Vanderbilt, *Phys. Rev. Lett.* **89**, 117602 (2002).
- [10] P. Umari and A. Pasquarello, *Phys. Rev. Lett.* **89**, 157602 (2002).
- [11] R. Resta, *J. Phys.: Condens. Matter* **14**, R625 (2002).
- [12] C. Sgiovello, M. Peressi, and R. Resta, *PRB* **64**, 115202 (2001).
- [13] P. Fernandez, A. Dal Corso, and A. Baldereschi, *Phys. Rev. B* **58**, R7480 (1998).
- [14] R. W. Nunes and D. Vanderbilt, *Phys. Rev. Lett.* **73**, 712 (1994).
- [15] F. Giustino and A. Pasquarello, *Phys. Rev. B* **71**, 144104 (2005).
- [16] N. Marzari and D. Vanderbilt, *Phys. Rev. B* **56**, 12847 (1997).
- [17] N. Marzari, D. Vanderbilt, and M. C. Payne, *Phys. Rev. Lett.* **79**, 1337 (1997).
- [18] M. Stengel and N. A. Spaldin, cond-mat/0506389 (2005).
- [19] J. Neugebauer and M. Scheer, *Phys. Rev. B* **46**, 16067 (1992).
- [20] M. Stengel and A. De Vita, *Phys. Rev. B* **62**, 15283 (2000).
- [21] R. Car and M. Parrinello, *Phys. Rev. Lett.* (1985).
- [22] J. Vandevondele and A. De Vita, *Phys. Rev. B* **60**, 13241 (1999).
- [23] J. A. Perdew and A. Zunger, *Phys. Rev. B* **23**, 5048 (1981).
- [24] N. Troullier and J. L. Martins, *Phys. Rev. B* **43**, 1993 (1991).
- [25] L. Kleinman and D. M. Bylander, *Phys. Rev. Lett.* **48**, 1425 (1982).
- [26] S. G. Louie, S. Froyen, and M. L. Cohen, *Phys. Rev. B* **26**, 1738 (1982).

[27] We use a Gaussian filter to avoid the spurious identification of nodes of the wavefunction in a region close to its center.

[28] The sawtooth functions are constructed in reciprocal space in order to avoid Fourier aliasing errors and preserve analytical gradients.

[29] The resulting operator is Hermitian and the method is variational if and only if each Wannier-like state is strictly localized in $x \in [r_n - L/4; r_n + L/4]$, while otherwise the error can be systematically (and exponentially) reduced by increasing the thickness of the dielectric layer. In practice the Wannier functions cannot be made to be strictly confined within a standard plane-wave pseudopotential calculation, unless more exotic algorithms are used [13]. In order to correct for the non-Hermiticity of the Hamiltonian, which could cause convergence problems, we introduce a further small term which vanishes in the ideal, mathematically localized case:

$$\hat{H}^0 \mathbf{j}_i = \frac{E}{2} \sum_j \mathbf{j}_i \mathbf{j}_i \mathbf{w}_j \mathbf{j}_j (\mathbf{F}_j - \mathbf{F}_i) \mathbf{j}_i \mathbf{i}:$$

This way we could always achieve optimal convergence in our calculations.

[30] We note that the method is no means limited to metallic systems, and for purely insulating materials it is even easier to apply. In insulators, either with homogeneous or layered structures, our method is expected to provide a significant improvement over the customary Berry-phase-based approach concerning the convergence properties with respect to the supercell length L [18].

[31] Our calculations were performed within the local density approximation [23], by using norm-conserving Troullier and Martin [24] pseudopotentials in the Kleinman and Bylander [25] form. A non-linear core correction [26] was adopted for Mg. We used the theoretical in-plane lattice constant of MgO ($a_0 = 7.8$ a.u.), and a plane-wave cutoff of 70 Ry.